

ments.

Note added.—We have directly observed critical attenuation in EuO above T_c at a frequency of 235 kHz. The critical contribution to Γ is approximately 500 sec^{-1} at T_c . Using the measured critical attenuation and dispersion at $\epsilon = 10^{-3}$ and Eqs. (3) and (4), we estimate $\tau_c^{-1} \approx 1.5 \times 10^6 \text{ sec}^{-1}$, within a factor of 3. This result for τ_c^{-1} is consistent with high- and low-frequency acoustic measurements in EuO and reduces further the uncertainty in the magnitude of the critical relaxation rate.

*Work supported in part by the National Science Foundation under Grant No. GH33750 at the University of Illinois.

¹Y. Shapira and T. B. Reed, *J. Appl. Phys.* **40**, 1197 (1969).

²B. Lüthi and R. J. Pollina, *Phys. Rev. Lett.* **22**, 717 (1969).

³D. L. Huber, *Phys. Rev. B* **3**, 836 (1971).

⁴C. Zener, *Phys. Rev.* **52**, 230 (1937), and **53**, 90 (1938).

⁵B. Golding, *Phys. Rev. Lett.* **27**, 1142 (1971), and *J. Appl. Phys.* **42**, 1381 (1971).

⁶M. B. Salamon, B. Golding, and E. Buehler, to be published.

⁷A. Kornblit, G. Ahlers, and E. Buehler, to be published.

⁸It has been pointed out [K. Kawasaki and A. Ikushima, *Phys. Rev. B* **1**, 3143 (1970)] that in EuO there should actually be coupling of sound partially to energy fluctuations and partially to order-parameter fluctuations. No conclusive evidence for coupling to order-parameter fluctuations in magnetic insulators has been observed and the apparent absence of this interaction remains an unresolved problem in understanding critical attenuation of sound.

⁹K. Kawasaki, *Phys. Lett.* **29A**, 406 (1969), and *Int. J. Magn.* **1**, 171 (1971).

¹⁰B. Golding, *Phys. Rev. Lett.* **20**, 5 (1968).

¹¹T. J. Moran and B. Lüthi, *Phys. Rev. B* **4**, 122 (1971).

¹²Kawasaki and Ikushima, Ref. 8.

¹³Although the present measurements obtain the $\langle 110 \rangle$ Young's modulus velocity, and in Ref. 2 the $\langle 110 \rangle$ longitudinal plane-wave velocity was measured, the thermodynamic velocity changes associated with either mode near T_c differ by no more than a factor of 2, which is not significant for our estimate of τ_c^{-1} .

¹⁴This dispersion limit should not be confused with the $\Delta v/v$ quoted by Lüthi and Pollina (Ref. 2). In their data analysis, Fig. 3 of Ref. 2, they apparently take $\Delta v/v \equiv [v(\omega) - v_\infty]/v$, whereas in their Eq. (4) [which follows from our Eq. (4)], $\Delta v/v \equiv [v(\omega) - v_0]/v$.

¹⁵In an earlier interpretation of the high-frequency measurements (Ref. 2), τ_D^{-1} was assumed to dominate the relaxation rate τ_c^{-1} .

¹⁶See, for example, B. Golding and M. Barmatz, *Phys. Rev. Lett.* **23**, 223 (1969).

¹⁷B. S. Berry, *J. Appl. Phys.* **26**, 1221 (1955).

Plasmon Observation Using X Rays*

K. L. Kliewer† and H. Raether

Institut für Angewandte Physik der Universität Hamburg, 2 Hamburg 36, Germany

(Received 30 January 1973)

We have investigated the problem of plasmon observation using high-energy photons within the context of the random phase approximation. It is shown that the experimental results from a study of Be by Miliotis can be readily understood from this point of view. It is further shown that these results include both collective and single-particle effects and that the collective effects persist well beyond the "critical wave vector." We discuss the concept of a critical wave vector.

Observations of plasmons in experiments which can, in analogy with electron energy loss, be described as photon energy loss have now been reported by a number of workers.^{1,2} Perhaps the most detailed study to date has been that of Miliotis² on Be. He observed that the height of the plasmon peak increased sharply with increasing q ($\hbar q$ is here the momentum transfer) at low q , reached a maximum, and then decreased slowly at higher q values, while the width of the plas-

mon line was roughly proportional to q^2 . In addition, the plasmon dispersion curve, while satisfying the well-known relation $\omega - \omega_p \propto q^2$ for small q , bent over for larger values of q and showed little dependence of ω on q . This region of little dispersion occurred for q values well beyond q_c , the critical value of q , leading Miliotis to conclude that "plasmons" appear where they are unexpected. We will show that all of the results of the experiment of Miliotis can be un-

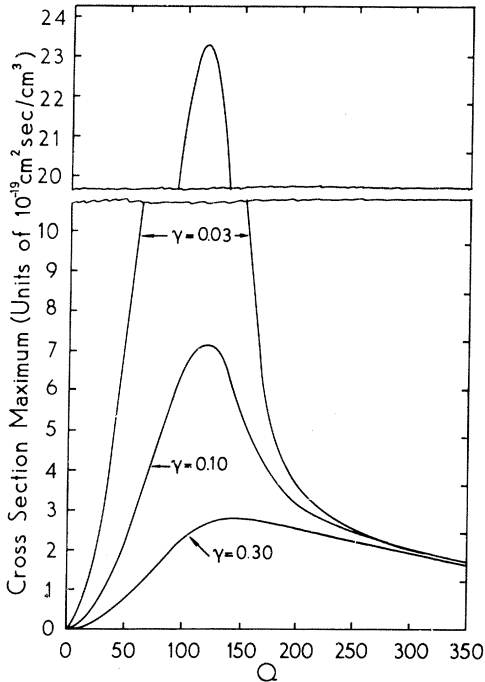


FIG. 1. Peak value of the cross section as a function of Q . The cross sections were calculated for an incident photon energy of 8.91 keV corresponding to the $K\beta$ line of copper.

derstood qualitatively within the context of the random phase approximation (RPA).

Our starting point is the RPA expression for the cross section for elementary excitation production by an unpolarized photon beam,³

$$d^2\sigma/d\Omega_s d\omega = A(1 - \frac{1}{2}\sin^2\theta)\omega_p^2 Q^2 \times \text{Im}[-1/\epsilon_l(Q, \Omega)], \quad (1)$$

where ω_p is the plasma frequency, $Q = qc/\omega_p$ is the dimensionless wave vector (c is the velocity of light), $\Omega = \omega/\omega_p$ is the dimensionless frequency, $d\Omega_s$ is the solid angle element, θ is the photon scattering angle associated with momentum transfer $\hbar q$, $\epsilon_l(Q, \Omega)$ is the longitudinal dielectric function. The constant $A = (e^2/mc^2)^2 \hbar (4\pi^2 c^2 e^2)^{-1}$ has the value $1.023 \times 10^{-56} \text{ sec}^3 \text{ cm}^2/\text{cm}^3$. The presence of Q^2 in Eq. (1) means that large- Q contributions to $\text{Im}(-1/\epsilon_l)$ will be strongly enhanced.

Since the magnitude of the damping significantly affects our results, we have used for ϵ_l a generalization⁴ of the Lindhard electron-gas dielectric function which incorporates the effects of damping through an effective electron lifetime τ . We characterize the damping with the damping parameter $\gamma = (\omega_p \tau)^{-1}$. The electron gas can be de-

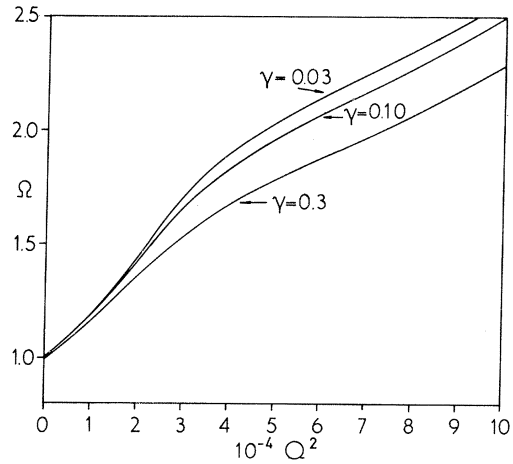


FIG. 2. Frequency Ω at which the peaks in the cross section occur as a function of Q^2 .

scribed by the parameter Δ , the ratio of the plasma energy $\hbar\omega_p$ to the Fermi energy.⁵ To simulate Be we have chosen $\Delta = 1.29$ such that r_s (the radius of a sphere containing one electron in units of the Bohr radius for hydrogen) = 1.88 and $\hbar\omega_p = 18.3 \text{ eV}$.

Let us consider initially $\gamma = 0.03$. The calculation was done by fixing Q and then examining the cross section as a function of Ω . The maximum value of the cross section is seen in Fig. 1 to rise steeply as Q increases from zero, to peak in the vicinity of $Q = 120$, and then to drop sharply to a slowly decreasing function of Q for $Q \geq 200$. The frequency at which the maximum in the cross section occurs is plotted in Fig. 2 as a function of Q^2 . For low Q , it is apparent that the peak in the cross section is due to plasmons. The frequency of the maximum coincides with the frequency for which the real part of ϵ_l is zero and is seen in Fig. 2 to increase somewhat more rapidly than quadratically in Q , as is appropriate for the RPA.⁶ However, for larger Q the slope of this curve decreases significantly. To provide an understanding of what is taking place, we follow the process as Q increases. For very low Q , the plasmons totally dominate $\text{Im}(-1/\epsilon_l)$ and thus the cross section. The half-width of the cross-section peak (shown in Fig. 3) is just γ . However, as Q increases the single-particle excitations, occurring on the low-frequency side of the plasmons, begin to show up in the cross section through an asymmetric broadening of the plasmon line.⁷ That is, the half of the half-width on the low-frequency side becomes larger than the half on the high-frequency side. This effect

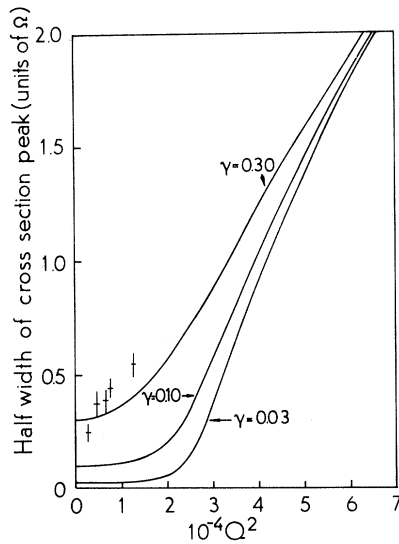


FIG. 3. Half-width (full width at half-maximum) of the cross-section peak in units of Ω as a function of Q^2 . The crosses are the data points of Miliotis (Ref. 2) plotted using the variables $\Omega = \omega/\omega_{px}$ and $Q = qc/\omega_{px}$ with $\hbar\omega_{px} = 19.4$ eV, the experimental result of Miliotis for the plasma frequency.

becomes noticeable for $Q^2 \sim 2.0 \times 10^4$, and, for $2.3 \times 10^4 \leq Q^2 \leq 7.3 \times 10^4$, the low-frequency part of the half-width is more than twice as large as the high-frequency part.⁸ Although, for these values of Q , the broad peak associated with the single-particle excitations contributes somewhat to this asymmetry, the principal cause is the superposition of a significant plasmon contribution upon the single-particle peak.

If the damping is increased so $\gamma = 0.10$, the magnitude of the cross-section peak is seen in Fig. 1 to decrease significantly only for $Q \lesssim 200$, indicating that the magnitude of the damping affects the contribution of the collective excitation much more than it does the contribution of the single-particle region. The frequency of the cross-section peak (Fig. 2) decreases for $Q^2 \gtrsim 3 \times 10^4$ since the maximum plasmon contribution to the cross section is now reduced, and thus the single-particle excitations, which tend to lower the frequency of the peak associated with the plasmons, are now relatively more important than for $\gamma = 0.03$. In addition, the asymmetry of the cross-section peak is reduced. These trends continue when the damping is further increased to $\gamma = 0.3$.

We have included in Fig. 3 the half-width results from the experiment of Miliotis⁹ (see Fig. 5 of Ref. 2) to indicate that a damping value of

0.30 may be a bit low but appears to represent the experimental results adequately, particularly in view of the approximate method used for obtaining these experimental half-width results and also the fact that interband effects, which significantly affect the effective value of γ and thus the plasmon peak shape,^{6,10} have not been included in the calculations. The shape of our maximum cross-section curve for $\gamma = 0.30$ agrees well with that of Fig. 6 of Ref. 2. The maximum in this curve occurs for $Q \sim 140$ theoretically and $Q \sim 120$ experimentally.⁹ Our curve of the frequency for which the maximum cross section occurs does not bend over as much as the experimental curve for large Q (compare Fig. 2 with Fig. 4 of Ref. 2). We do not feel that this is a serious deficiency in our results since there are both theoretical and experimental problems in this region. The theoretical cross section is so broad for large Q that the exact position of the maximum is not of much significance and could change markedly if, say, interband effects or corrections to the RPA were included. On the experimental side, the broad peak with which we are here dealing must be identified from experimental curves which include other physical phenomena as well. This is no simple matter and could lead to significant errors. So we conclude that the experimental results of Miliotis are readily understandable from the point of view of the RPA.

We have made additional calculations for various values of Δ between 1 and 2. The results do not differ qualitatively from those for $\Delta = 1.29$. We have also repeated our calculations using the dielectric function of Kliewer and Fuchs.¹¹ The results differ in detail from those obtained above, but not in physical content.

We turn now to a consideration of the concept of a critical wave vector q_c . Such a quantity has been utilized to indicate the q value at which plasmon damping begins to increase significantly as a result of decay into single-particle excitations (Landau damping) and also as a point of separation between low- q collective effects and high- q single-particle effects. The definition¹²

$$q_c = \omega_p/v_F = 0.47r_s^{1/2}k_F, \quad (2)$$

with v_F the Fermi velocity and k_F the Fermi wave vector, yields the value $Q_c = 134$ for Be in our dimensionless units. This q_c marks only in an approximate way a point of physical significance relating to the excitations of the electron gas, whereas defining q_c as the value of q for which the plasmon dispersion curve enters the single-

particle excitation region, the front edge of which is given by

$$\omega = (\hbar/2m)q^2 + v_F q, \quad (3)$$

neglecting damping effects, indicates clearly its role as the indicator of the onset of Landau damping. Characterizing the plasmon by the peak in $\text{Im}(-1/\epsilon_l)$, this latter definition of q_c involves following the peak position (Fig. 2) and determining where it crosses the line of Eq. (3).¹³ Consider $\gamma=0.03$. Using this criterion we find a critical Q of 147, at which point the half-width of the cross-section peak (Fig. 3) is about 3 times the intrinsic width of 0.03. For $\gamma=0.10$ we find the critical Q to be 142 where the half-width is approximately twice the $Q=0$ value. When $\gamma=0.30$, the critical Q is 133 and the half-width about 1.7 times that for $Q=0$. These half-width increases indicate that this criterion provides a reasonable indication of the Q values at which the damping begins to increase significantly. However, these critical values of Q are sufficiently close to that of criterion (2) that there is no point in attempting to make a case for the superiority of either. But what about the possible role of the critical wave vector as a boundary between collective and single-particle effects? For large Q , there is no definitive way to separate the collective from the single-particle effects. However, if we argue, as our results suggest, that the magnitude of the damping affects principally the collective effects, then Fig. 2 indicates significant plasmon contributions to well beyond $2Q_c$. Of course, one might argue that for such large values of Q the plasmon is so strongly affected by the single-particle region that the resultant effect is largely single-particle in character. However, such a claim cannot be made for wave vectors as low as $Q=134$, the critical wave vector of criterion (2). We conclude, then, that the critical wave vector of ordinary usage is a useful indicator of the onset of strong plasmon damping, and that significant collective effects persist to wave vectors well beyond this critical value.

It was noted above only in passing that the contribution to the cross section arising from the single-particle excitations forms what is generally referred to as the Compton band. This aspect of the Compton effect has not been emphasized since our primary interest in the present note is the plasmon. We will discuss elsewhere

the single-particle effects and, in particular, the fashion in which the cross section associated with them changes, as Q increases, into a function peaked at the energy difference given by the standard Compton equation.

The use of x rays or, perhaps, synchrotron radiation appears to be an excellent technique for investigating plasmon properties in the range of wave vectors where it is difficult to obtain accurate results from electron energy-loss experiments.¹⁴ For such wave vectors, this technique should serve as an effective complement to that of resonant excitation of plasmons in thin films, which has been used for the determination of plasmon dispersion curves in silver¹⁵ and potassium.¹⁶

*Work supported in part by the U. S. Atomic Energy Commission.

†On faculty leave from Ames Laboratory—U. S. Atomic Energy Commission and Department of Physics, Iowa State University, Ames, Ia. 50010.

¹N. G. Alexandropoulos, *J. Phys. Soc. Jap.* **31**, 1790 (1971).

²D. M. Miliotis, *Phys. Rev. B* **3**, 701 (1971).

³D. Pines, *Elementary Excitations in Solids* (Benjamin, New York, 1964), p. 207.

⁴N. D. Mermin, *Phys. Rev. B* **1**, 2362 (1970).

⁵Expressions for all parameters of the electron gas in terms of Δ appear in R. Fuchs and K. L. Kliewer, *Phys. Rev. B* **3**, 2270 (1971).

⁶M. S. Haque and K. L. Kliewer, *Phys. Rev. Lett.* **29**, 1461 (1972), and *Phys. Rev. B* **7**, 2416 (1973).

⁷The contribution to the cross section from the single-particle excitations, reflecting the consequences of the Pauli principle, forms the Compton band.

⁸The plasmon dispersion curve enters the single-particle excitation region for $Q \sim 140$ as is discussed below.

⁹The experimental results have been translated into our dimensionless variables via $\Omega = \omega_{px}$ and $Q = qc/\omega_{px}$, with $\hbar\omega_{px} = 19.4$ eV (see Ref. 2).

¹⁰P. Zacharias, *Z. Phys.* **256**, 92 (1972).

¹¹K. L. Kliewer and R. Fuchs, *Phys. Rev.* **181**, 552 (1969).

¹²Ref. 3, p. 100.

¹³An approximate version of this criterion, without the inclusion of damping effects, is discussed in Ref. 3, p. 148.

¹⁴Evidence that this technique can provide information about surface plasmons as well has been obtained by C. Koumelis and D. Leventouri, *Phys. Rev. B* **7**, 181 (1973).

¹⁵I. Lindau and P.-O. Nilsson, *Phys. Scri.* **3**, 87 (1971).

¹⁶M. Anderegg, B. Feuerbacher, and B. Fitton, *Phys. Rev. Lett.* **27**, 1565 (1971).